Pergamon

Tetrahedron: *Asymmetry* 11 (2000) 2495–2507

TETRAHEDRON: *ASYMMETRY*

Atropdiastereoisomers of ellagitannin model compounds: configuration, conformation, and relative stability of D-glucose diphenoyl derivatives[1]

Stefan Immel[a,*] and Karamali Khanbabaee[b]

[a]*Institut für Organische Chemie, Technische Universität Darmstadt, Petersenstraße 22, D-64287 Darmstadt, Germany*
[b]*Fachbereich Chemie und Chemietechnik der Universität-GH Paderborn, Warburgerstraße 100, D-33098 Paderborn, Germany*

Received 18 April 2000; accepted 9 May 2000

Abstract

Conformational analysis reveals a remarkable rigidity of 2,3-, 4,6-, 3,6-, and 2,4-*O*-(*S*)- and (*R*)-diphenoyl (DP) bridged methyl β-D-glucosides, which were used as model compounds to evaluate the atropisomeric features of the natural ellagitannins, which possess at least one hexahydroxydiphenoyl (HHDP) moiety. The 2,3- and 4,6-*O*-(*S*)-DP bridged glucosides with $^4C_1$ pyranose geometries are thermodynamically more stable than their (*R*)-DP counterparts, whilst in the 3,6- and 2,4-*O*-linked series with $^1C_4$ glucopyranose geometries the (*R*)-DP configuration is preferred. The chiral scaffold of glucose exerts a strong atropdiastereoselective effect onto the diphenoyl units, which is mediated through 10- to 12-membered rings via ester linkages. The calculated results not only explain the observed (*S*)-diastereoselectivity of di-esterification reactions of suitably protected racemic hexaoxydiphenic acids with 4,6-unsubstituted D-glucopyranose derivatives, but also correlate the observed configuration of axially chiral HHDP-moieties of natural ellagitannins with conformational parameters.

1. Introduction

Ellagitannins constitute members of a large class of polyphenolic natural products that can be obtained by extraction from higher plants.[2] These extracts are widely used in folk medicine, leather and wine industry, and the tannin-components exhibit a broad range of biological activities.[2] The common structural element of the ellagitannins is a hexahydroxydiphenoyl (HHDP) unit located at the 2,3-, 4,6-, 1,6-, 3,6-, and/or 2,4-positions of the D-glucopyranose core.

The axially chiral HHDP-units of the 2,3- and 4,6-*O*-HHDP ellagitannins exhibit almost invariably the (*S*)-configuration with only very few exceptions (Cercidinin A and B,[3] Cuspinin,[3] and Platycaryanin D[4]) amongst more than 500 structurally characterized compounds (Fig. 1).[2,5]

* Corresponding author. E-mail: lemmi@sugar.oc.chemie.tu-darmstadt.de

0957-4166/00/$ - see front matter
PII: S0957-4166(00)00179-8

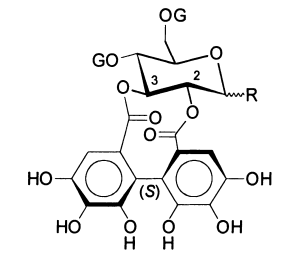

2,3-*O*-HHDP ellagitannins

1 R = β-OG Pterocarinin C
2 R = OH Praecoxin B
3 R = β-OG Mahtabin A (*R*)-HHDP
4 R = OH Pariin M (*R*)-HHDP

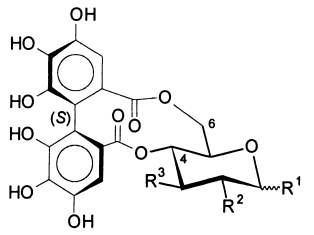

4,6-*O*-HHDP ellagitannins

5 R^1 = β-OG $R^{2,3}$ = OH Strictinin
6 R^2 = OG $R^{1,3}$ = OH Hippomanin A
7 R^3 = OG $R^{1,2}$ = OH Gemin D
8 $R^{2,3}$ = OG R^1 = OH Tellimagrandin I
9 R^1 = β-OG $R^{2,3}$ = OG Tellimagrandin II

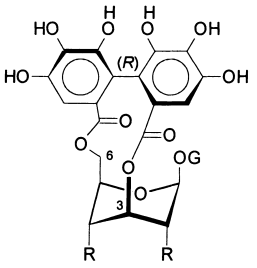

3,6-*O*-HHDP ellagitannins

10 R = OH Corilagin
11 R,R = Geraniin

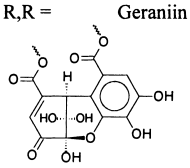

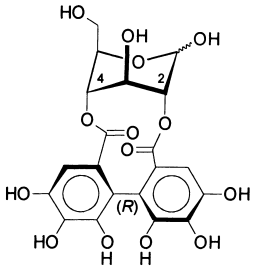

2,4-*O*-HHDP ellagitannin

12

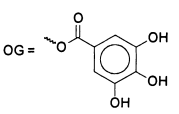

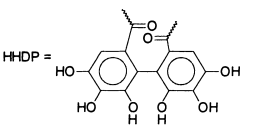

Figure 1. Chemical formulas of 2,3-, 4,6-, 3,6-, and 2,4-*O*-hexahydroxydiphenoyl (HHDP) glucosides (ellagitannins) with axial chirality of the HHDP moieties

Recently, it was shown that the postulated structures for the unusual ellagitannins Cercidinin A and B,[3] each possessing a 2,3-(*R*)-HHDP unit, are incorrect and must be revised.[6]

Prominent examples for the 2,3-*O*-(*S*)-HHDP ellagitannins are Pterocarinin C **1** and Praecoxin B **2**,[7] their non-natural, unusual (*R*)-HHDP counterparts Mahtabin A **3** and Pariin M **4** have become accessible in enantiomerically pure form through ring forming di-esterification of the *o*-nitrobenzyl 4,6-*O*-benzylidene-β-D-glucoside with racemic hexabenzyloxydiphenic acid.[6] Total syntheses of the natural 4,6-*O*-(*S*)-HHDP ellagitannins **5**–**7**[8,9] were achieved through unexpectedly highly atropdiastereoselective di-esterification reactions of racemic hexabenzyloxydiphenic acid with different 4,6-unsubstituted D-glucopyranose derivatives, exclusively leading to the corresponding 4,6-*O*-(*S*)-HHDP diastereomers. In contrast, in the same reactions the (*R*)-component of the racemic hexabenzyloxydiphenic acid gave rise to the formation of oligomers through the possible intermolecular competition pathway only.[8–10] On the other hand, the naturally occurring ellagitannins in which the HHDP-units are attached to the 3,6- (Corilagin **10**[11] and Geraniin **11**[12,13]) or 2,4-positions[14] **12** of glucopyranose exhibit (*R*)-HHDP configuration,[2] although the latter invariably undergo further biochemical transformations under physiological conditions.[2]

The highly atropdiastereoselective formation of the ellagitannins from their biochemical gallotannin precursors has been explained through conformational preferences of the galloyl residues, and strain in the transition states of the oxidative coupling reactions between galloyl esters.[2,12,15–17] However, despite the wide-spread occurrence of polyphenolic compounds of tannin class natural products, very little structural data on gallotannins or ellagitannins at atomic resolution is available through crystal structure analysis; the only examples available from the Cambridge Crystallographic Database[18] are Geraniin **11**[19] and methyl 4,6-*O*-benzylidene-2,3-*O*-(*S*)-hexamethoxydiphenoyl-α-D-glucopyranoside **13**.[20]

As chemical syntheses of the ellagitannins proceed either via oxidative coupling of galloyl residues in galloylated glucose substrates, or alternatively through di-esterification of methyl- or benzylether-protected enantiopure or racemic hexahydroxydiphenic acid with appropriately substituted D-glucosides,[2] stereocontrol of these reactions is of fundamental importance. Therefore, we have undertaken a molecular modeling study of some ellagitannin model compounds with the aim of obtaining structural models on an atomic level, and to explain the relative stabilities of the various (*R* and *S*)-HHDP diasteromers under equilibrium conditions.

2. Results and discussion

We chose the compounds **14**–**21** (Fig. 2) as a starting point for our study on the different types of ellagitannins. The hydroxyl groups of the HHDP- and galloyl-residues were omitted in order to reduce the number of local minima on the energy potentials surfaces of the ellagitannins originating from different OH-rotamers (→diphenoyl and benzoyl-substituents). This simplification also avoids conformational artifacts stabilized by strong intramolecular hydrogen bonds, as the geometry analyses were carried out for the isolated molecules only without the explicit incorporation of a solvent; for the same reason, the methyl β-D-glucosides were considered only. Starting geometries were generated for all types of 2,3-, 4,6-, 3,6-, and 2,4-type linkages, and both (*S*)- and (*R*)-diphenoyl (DP) atropdiastereoisomers, respectively. In the first class of compounds, the 4- and 6-OH groups of glucose were 'blocked' by benzoyl groups as mimics for the galloyl residues (vide supra).

In each case, the conformational space was explored by a mixed molecular dynamics (MD) and molecular mechanics (MM) approach, applying a full energy optimization to 5000 structures extracted along a 500 ps MD trajectory (for details, see Experimental). As was established through monitoring a number of molecular parameters along the MD runs, this methodology did not only produce glucose conformations other than $^4C_1$ or $^1C_4$, but it also generated a large number of conformers of the diphenoyl ring system. The atropstereochemical configuration of all diphenoyl units was retained during all MD simulations, and no (*S*)↔(*R*) transitions were recorded. The fully relaxed, global energy-minimum structures obtained were used in this report, and for each model compound some characteristic geometry parameters (cf. Fig. 2) are listed in Table 1.

2.1. 2,3-O-*Diphenoyl glucosides* ***14*** *and* ***15***

The global energy-minimum structures of **14** and **15** are shown in Fig. 3, with **14** being about 7.4 kJ/mol more stable than **15** (cf. Table 1). The glucopyranose units adopt standard $^4C_1$ ring geometries as evidenced by their Cremer-Pople ring puckering parameters[21] (cf. Table 1), and the

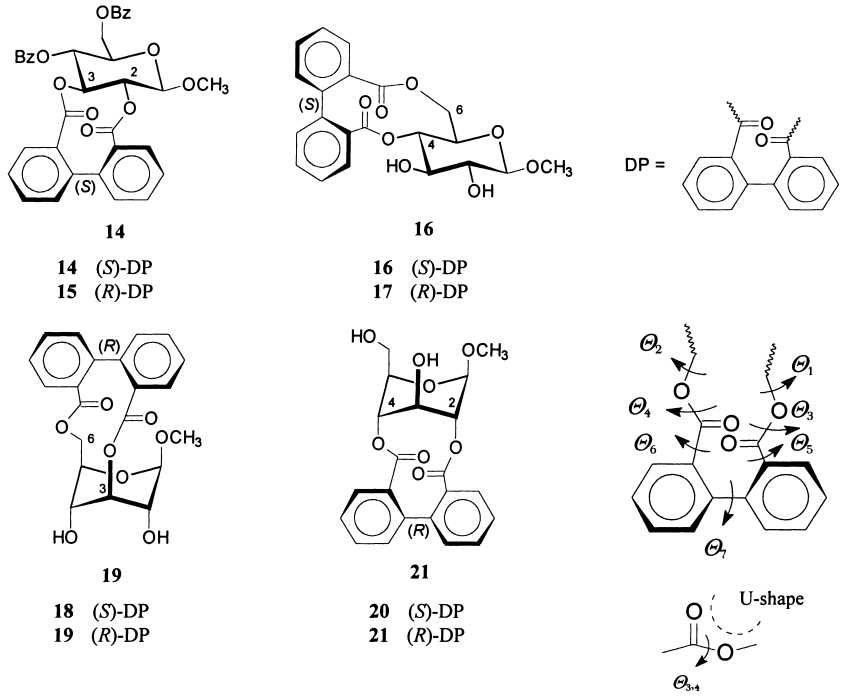

Figure 2. Methyl 2,3-, 4,6-, 3,6-, and 2,4-*O*-(*R*,*S*)-diphenoyl-β-D-glucosides **14**–**21** used as model structures for evaluating the conformational properties of ellagitannins (DP = diphenoyl). On the right, some ring torsion angles Θ_1–Θ_7 used in the geometry analysis are given. Θ_1 and Θ_2 define the mode of attachment of the diphenoyl-unit to the glucopyranose ring. The preferred U-shape of both ester groups is characterized by Θ_3 and Θ_4 with ideal values of approximately 0°; Θ_5 and Θ_6 denote the inclination of the carbonyl groups towards the phenyl rings (ideal values 0° and ±180° for conjugated π-systems). The atropisomeric diphenoyl units display torsion angles Θ_7 of opposite sign (*R*: negative, *S*: positive values); Θ_7 is approximately equivalent to the tilt angle between the phenyl rings

conformational preferences of the 10-membered diphenoyl ring system are largely determined by its rather rigid *trans*-type linkage to the pyranose scaffold. The two ester groups display a highly characteristic tendency to maintain an U-shape (Fig. 2), although the torsion angles Θ_3 and Θ_4 indicate about a 30° deviation from the ideal geometry for **14** (Table 1). In **15**, the glucose 2-OCO-ester group is forced by the (*R*)-DP residue into a strained *trans*-type conformation with $\Theta_3 \approx 140°$. In both compounds **14** and **15**, the carbonyl groups are inclined by about 40–50° (Θ_5 and Θ_6) relative towards the planes of phenyl ring π-systems. The phenyl rings of the DP-units are tilted towards each other by about 50–60° (torsion angle Θ_7 in Table 1, positive values of Θ_7 indicating (*S*)-DP units and negative (*R*)-DP configurations). Most notably, the ester groups tend to adopt an antiparallel arrangement of their C=O dipoles (angles φ of 150–165°), whereas the tilt angles τ indicate an almost parallel (stacked) alignment of the planes formed by the C-COO-atoms of each ester fragment. These geometry parameters clearly reveal the torsion angle Θ_3 as the main reason for the lower stability of **15** as compared to **14**.

This notion is further substantiated through color-coded projection of the force-field derived split-terms of strain energy originating from angle- and torsion-bending onto the ball-and-stick models of **14** and **15**. In Fig. 4, blue colors correspond to relaxed molecular fragments, whereas yellow to red colors indicate strain on distinct residues. In both cases, the type of ring-anellation

Table 1
Relative energies and selected geometry parameters calculated for the global energy-minimum structures of the ellagitannin model compounds **14**–**21**. For each type of 2,3-, 4,6-, 3,6-, and 2,4-*O*-diphenoyl bridged glucopyranose derivative, the (*S*)- and (*R*)-atropdiastereomers are listed; the *galacto*-configured compounds **23** and **24** lack naturally occurring counterparts amongst the ellagitannins, but were included for comparison (cf. text)

	compound	**14**	**15**	**16**	**17**	**18**	**19**	**20**	**21**	**23**	**24**
	linkage type	2,3-(*S*)	2,3-(*R*)	4,6-(*S*)	4,6-(*R*)	3,6-(*S*)	3,6-(*R*)	2,4-(*S*)	2,4-(*R*)	4,6-(*S*)[a]	4,6-(*R*)[a]
ΔH_{calc} [kJ/mol]	absolute	-	-	-	-	-	-	-	-	-	-
	relative	1245.	1238.	1158.	1153.	1145.	1172.	1125.	1130.	1150.	1159.
		4	0	7	2	3	4	3	9	9	5
		0.0	7.4	0.0	5.5	27.1	0.0	5.6	0.0	8.6	0.0
	conformation	$^4C_1$	$^4C_1$	$^4C_1$	$^4C_1$	$^1C_4$	$^1C_4$	$^1C_4$	$^1C_4$	$^4C_1$	$^4C_1$
pyranose	Q [Å]	0.545	0.615	0.556	0.557	0.490	0.528	0.543	0.543	0.577	0.545
Cremer-Pople	θ [°]	11.6	8.4	11.5	7.3	176.2	172.6	173.6	172.6	3.8	5.4
parameters[21]	ϕ [°]	37.8	243.8	341.2	285.1	208.0	31.2	43.3	317.8	288.1	21.9
torsion angles[b]	Θ_1 (C_{pyr}-C''$_{pyr}$-O-C)	-81.6	-84.3	-130.9	-162.8	73.2	75.2	-64.1	-68.9	164.5	128.8
[°]	Θ_2 (C'$_{pyr}$-C''$_{pyr}$-O-C)	-82.1	48.2	-111.8	91.5	118.3	125.2	58.1	63.7	116.8	115.3
	Θ_3 (C_{pyr}-O-C=O)	-32.7	136.9	-28.9	-116.0	53.9	0.1	-20.5	-166.0	130.5	26.4
	Θ_4 (C'$_{pyr}$-O-C=O)	-33.0	34.1	-30.5	18.8	28.6	40.5	-176.1	23.5	177.1	29.5
	Θ_5 (O=C-C_{dp}-C_{dp})	42.4	-44.6	49.2	-107.0	138.3	-43.5	63.5	-61.1	124.6	-47.6
	Θ_6 (O=C-C'$_{dp}$-C'$_{dp}$)	42.9	-50.9	36.9	-38.3	141.7	-33.6	49.9	-60.6	78.4	-38.9
	Θ_7(C_{dp}-C_{dp}-C'$_{dp}$-C'$_{dp}$)	48.9	-61.9	56.2	-74.6	90.8	-58.3	63.9	-70.1	114.6	-54.5
	ω (O_5-C_5-C_6-O_6)	43.7[c]	71.0[c]	-80.9	-170.7	-99.0	175.3	173.0[c]	167.6[c]	168.8	-173.9
angle [°]	φ (C=O / C=O)[d]	165.9	153.3	150.6	120.7	167.1	154.1	138.9	138.2	130.4	151.4
tilt angle [°]	τ (COO / COO)[e]	175.6	176.2	168.5	132.4	88.0	160.6	162.8	167.3	134.4	168.9

a) D-*galacto*-configuration. — b) C_{pyr} and C'$_{pyr}$ denote the pyranose positions linked to the diphenoyl moiety, i.e. C_{pyr} / C'$_{pyr}$ = C_2 / C_3 for **14** and **15**; C_4 / C_6 for **16, 17, 23,** and **24**; C_3 / C_6 for **18** and **19**; C_2 / C_4 for **20** and **21**; C_{dp} and C'$_{dp}$ refer to the diphenoyl unit. — c) torsion angle ω not part of the diphenoyl ring system in **14**, **15**, **20** and **21**. — d) angle between the bond vectors of the ester carbonyl groups. — e) tilt angle between the two planes defined by the ester groups (atoms C-COO).

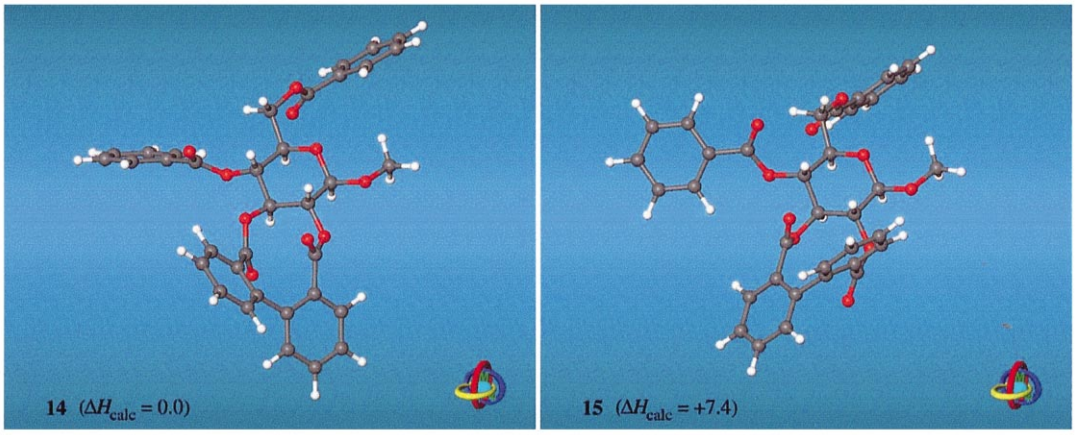

Figure 3. Ball-and-stick models of the global energy-minimum structures of the 2,3-*O*-(*S*)-DP **14** and (*R*)-DP **15** glucosides; calculated relative energies are given in kJ/mol

exerts strain on the position C-4 of the glucopyranose. In addition, **15** clearly displays through red colors internal strain centered around the 2-OCO ester. The rather rigid glucose unit serves as chiral strait-jacket, to which only a (*S*)-DP unit can be attached in a 'relaxed' conformation to the 2-O- and 3-O-groups, the atropstereochemical induction being mediated through the stiff ester groups in the attached ring.

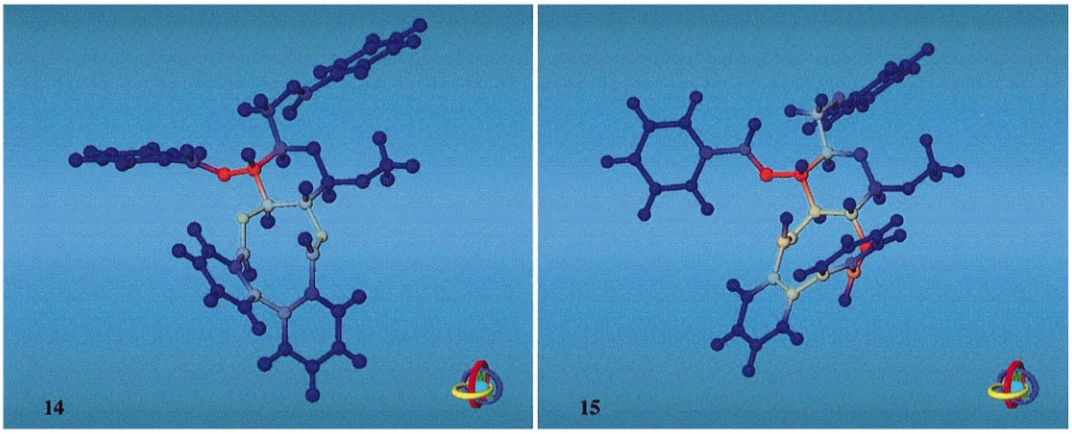

Figure 4. Color-coded projection of the force-field derived sum of split terms of angle- and torsion-bending strain energy onto ball-and-stick models of 2,3-*O*-(*S*)-DP **14** (left) and (*R*)-DP **15** (right) glucosides; blue colors indicate relaxed molecular parts, and yellow/green to red colors designate strained fragments (strain energies 0–5 kJ/mol); the mode of viewing corresponds to Fig. 3. The rigidity of both the pyranose and DP-ring systems, as well as the stiffness of the ester groups lead to a high energy conformation of the glucose 2-O-ester linkage in **15**

Some indications on the relevance of the computer-generated geometries are derived from comparison of **14** with the conformation of methyl 4,6-*O*-benzylidene-2,3-*O*-(*S*)-hexamethoxydiphenoyl-α-D-glucopyranoside **13** obtained from crystal structure analysis.[20] Superimposition of the common molecular fragments of **14** and **13** (Fig. 5) displays a high degree of correlation between the theoretically predicted and experimentally observed structures: in particular the ring linkage, the alignment of the ester groups, as well as the relative tilt of the phenyl rings are predicted accurately.

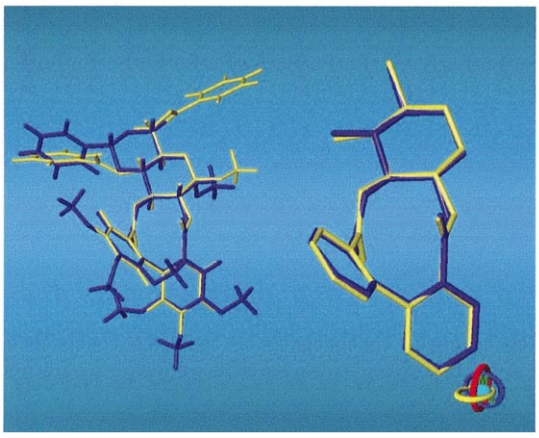

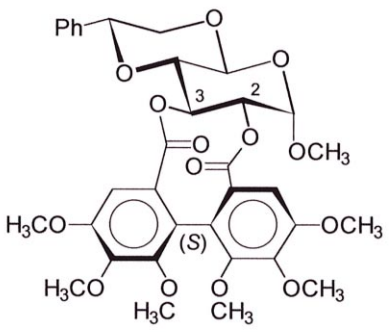

23

Figure 5. Superimposition of the computer-generated geometry of **14** (yellow model) with the solid-state conformation of methyl 4,6-*O*-benzylidene-2,3-*O*-(*S*)-hexamethoxydiphenoyl-α-D-glucopyranoside[20] (**13**, blue model). On the left, both structures are displayed entirely, whereas on the right only the common molecular fragments used for 3D-fitting are shown in enlarged form; the best-fit yielded a root mean square (RMS) deviation of $\sigma = 0.08$ Å for these atomic positions

2.2. 4,6-O-Diphenoyl glucosides **16** and **17**

In the 4,6-*O*-DP bridged glucosides **16** and **17** (Fig. 6), the same basic conformational effects as in the 2,3-*O*-DP series (**14** and **15**) are operative: the rather stiff U-shape of both ester groups, the preferred antiparallel C=O-dipole–dipole alignment, the conjugation of carbonyl and phenyl ring π-systems, as well as the tilt between the phenyl rings. In addition, the glucose 6-CH_2O-group is less flexible than it appears: of the three principal staggered conformations of the 6-C–O-linkage, the *trans–gauche* (*tg*)[22] form is commonly the least preferred one, as it is destabilized by 1,3-diaxial like repulsions between O-4 and O-6 (Scheme 1).[22,23] Although the *gauche–gauche* (*gg*) and *gauche–trans* (*gt*) forms[22] are usually equivalent in energy in non-cyclic glucose derivatives,[23] the latter becomes inaccessible in the 11-membered ring systems of the 4,6-*O*-DP glucosides **16** and **17** for sterical reasons. The *gg*-form[22] is realized in **16** ($\omega\approx$–80°, cf. Table 1), still allowing almost relaxed U-shaped ester linkages (Θ_3 and $\Theta_4\approx$–30°). As discussed above, a value of $\Theta_3\approx$–116° indicates a highly bent 6-OCO-ester linkage in **17**, and its strain is only partly relaxed through sacrificing the 6-O *gg*-form to a less preferred *tg*-geometry ($\omega\approx$–170° in **17**). However, superimposition of multiple low-energy conformers for both **16** and **17** (Fig. 7) indicates a lower flexibility of **16** as all ring fragments reside in a 'relaxed' state, whereas the strain in **17** (vide supra) allows for multiple conformations of the 6-C-OCO-fragments with different orientations of the ester carbonyl group. The data listed in Table 1 also indicates a less favorable alignment of the ester groups in **17** as compared to **16** (angles of $\varphi\approx$120° vs. 150° and tilts $\tau\approx$130° vs. 170° in **17** and **16**).

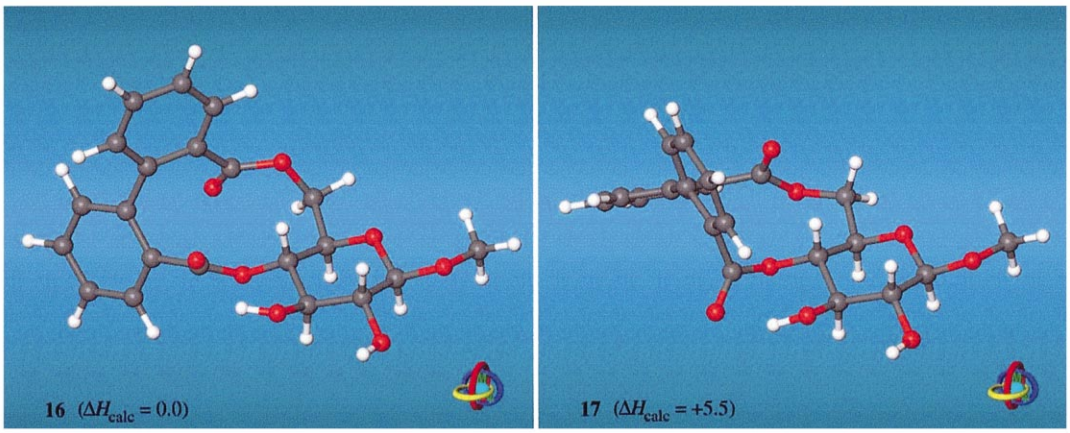

Figure 6. Ball-and-stick models of the global energy-minimum structures of the 4,6-*O*-(*S*)-DP **16** and (*R*)-DP **17** glucosides; relative energies are given in kJ/mol

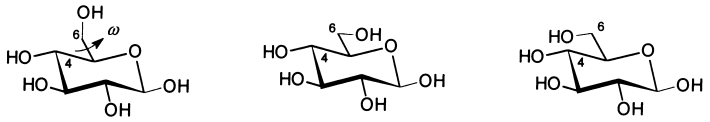

Scheme 1.

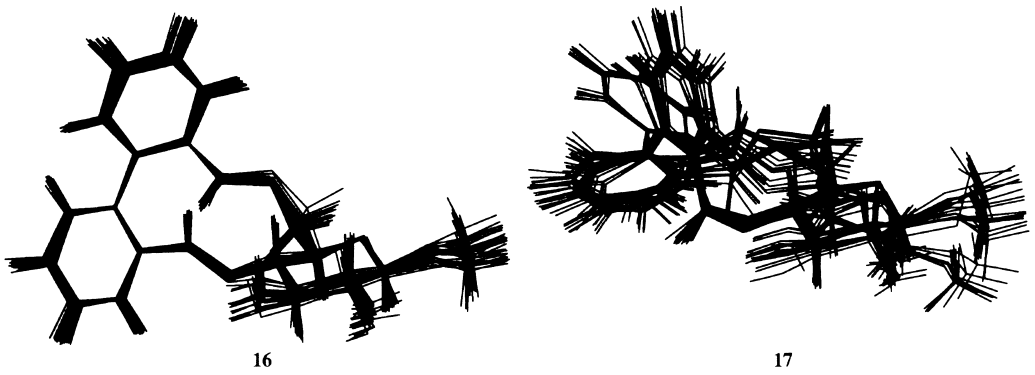

Figure 7. Superimposition of the 25 most stable geometries found within an energy range of approx. 0–10 kJ/mol above the global energy-minima for the atropdiastereomeric 4,6-*O*-DP glucoside model compounds **16** and **17**, respectively; the viewpoint relative to the glucopyranose ring is identical in both cases. The more stable (*S*)-DP compound **16** is remarkably rigid with rather stiff ring conformations. (*R*)-**17** displays some flexibility, and particularly the 6-CH_2-OCO ester carbonyl group adopts different orientations with almost equal energies (cf. text)

In Fig. 8, the calculated geometry of **16** is compared with the corresponding (*S*)-binaphthalene conformation in the crystal structure of racemic **22**:[24] although the 11-membered ring in the latter compound includes a Csp^2 carbonyl bridge head versus a 5-Csp^3 carbon in D-glucose, the 3D-fit displays very similar ring conformations in both compounds. In total, the geometry parameters obtained are consistent with preferred 4,6-*O*-(*S*)-DP D-glucose type linkages over (*R*)-DP geometries, and thus agree well with the absence of natural ellagitannins of the latter type.

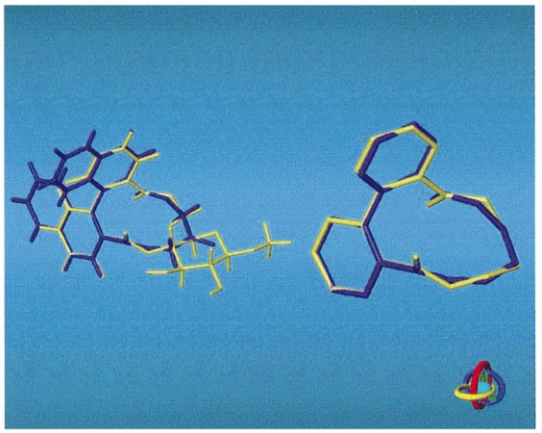

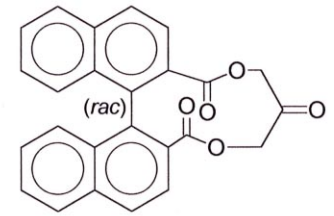

22

Figure 8. Superimposition of the 3D-structures of methyl 4,6-*O*-(*S*)-diphenoyl-β-D-glucoside (**16**) with the corresponding (*S*)-binaphthalene geometry extracted from the solid-state structure of racemic **22**,[24] the mode of viewing corresponds to Fig. 5. Despite the chemical differences of both compounds, the 11-membered rings display similar conformations with RMS deviations in the atomic positions of $\sigma \approx 0.1$ Å only

It is noteworthy, that the atropstereochemical induction on the DP-units strongly depends on the type of linkage and the configuration of the carbohydrate template: comparison of the 4,6-*O*-(*S*)-DP and 4,6-*O*-(*R*)-DP D-galactopyranosides **23** and **24**[25] with their D-glucose analogs **16** and **17** reveals opposite effects on the chirality of the DP-residues. The (*R*)-configuration of **24** is

about 8.6 kJ/mol more stable than the corresponding (*S*)-geometry (cf. Table 1 and Fig. 9). Due to the axial configuration at C-4 in D-galactose, the conformational preference of the 6-CH_2O-group is shifted from the *gg*- to the *tg*-form.[22]

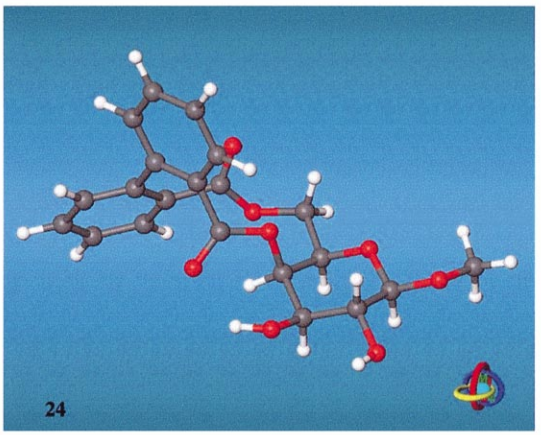

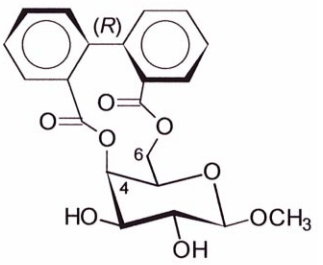

23 (*S*)-DP
24 (*R*)-DP

Figure 9. Global energy-minimum structure of 4,6-*O*-(*R*)-DP galactopyranoside **24** (left)

2.3. 3,6- and 2,4-O-Diphenoyl glucosides **18**–**21**

In both series of 3,6-*O*-DP (**18**, **19**) and 2,4-*O*-DP (**20**, **21**) bridged methyl β-D-glucosides, the glucose units are forced into $^1C_4$ chair geometries to affect ring closure (cf. Cremer–Pople ring puckering parameters[21] in Table 1); a behavior that is well-documented in the chemistry of 3,6-anhydro glucose derivatives.[26] Thus, the linkage positions as well as all other ring substituents adopt axial orientations on the pyranose ring, and in both 3,6-*O*-DP and 2,4-*O*-DP glucosides the (*R*)-DP configuration **19** and **21** is energetically preferred over the (*S*)-DP analogs **18** and **20** (cf. Table 1, and Figs. 10 and 11).

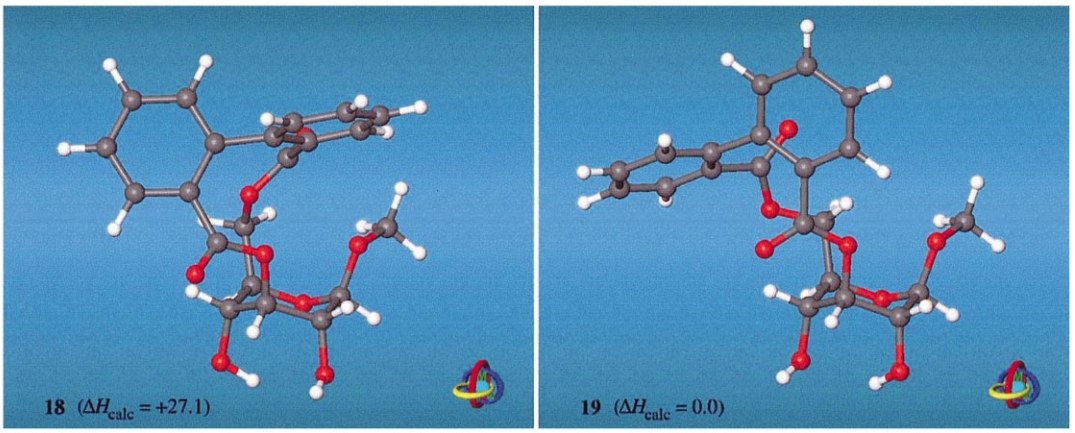

Figure 10. Global energy-minimum structures of the 3,6-*O*-(*S*)-DP **18** and (*R*)-DP **19** glucosides; relative energies are given in kJ/mol

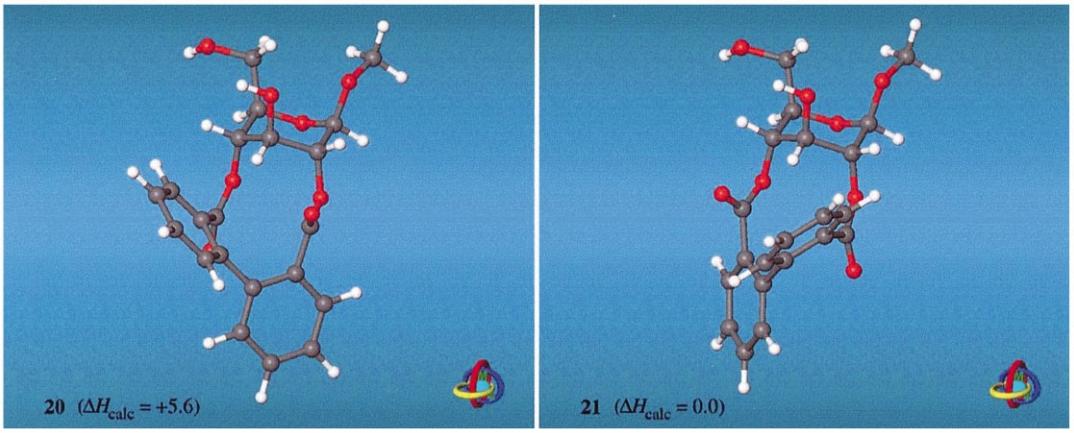

Figure 11. Global energy-minimum structures of the 2,4-*O*-(*S*)-DP **20** and (*R*)-DP **21** glucosides

As discussed above, it is the high tendency of the ester groups to maintain their characteristic U-shape, that transmits the chiral information of the carbohydrate backbone into the DP-residue, and thus induces their atropstereochemical configuration. Comparison of the calculated structure of **19** with the solid-state conformation of the natural ellagitannin Geraniin **11**[19] (Fig. 12) reveals very similar over all-shapes for both 3,6-*O*-(*R*)-DP ring systems, although the puckering of the pyranose ring is calculated to be smaller than found in the crystal structure of **11**.[19] However, the ring flattening effect observed in **19** is counterbalanced in **11** through an additional rigid linkage between the axial 2- and 4-OH groups of the D-glucoside core.

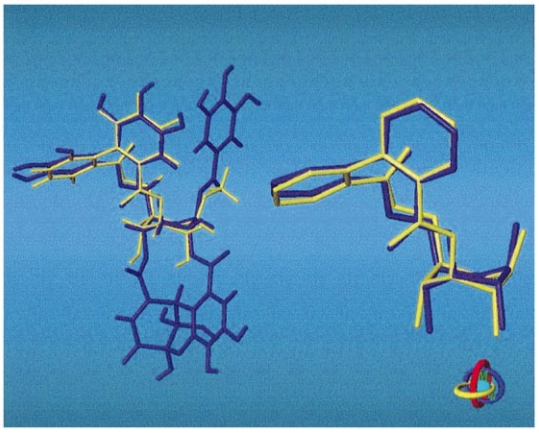

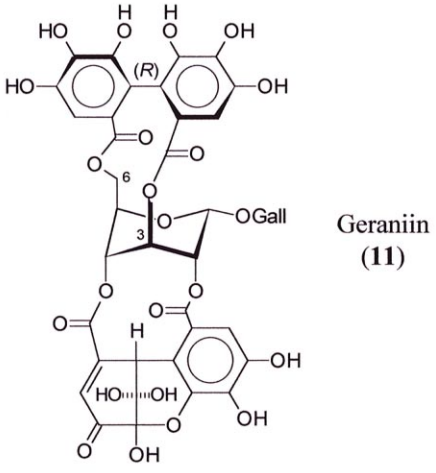

Geraniin
(11)

Figure 12. Superimposition of the energy-minimum structure **19** (yellow model) with the solid-state geometry of Geraniin **11**[19] (blue colors); the mode of viewing is analog to Figs. 5 and 8 (RMS deviation of $\sigma = 0.11$ Å for all equivalent atomic positions)

It is noteworthy, that in neither the 2,4-*O*-(*S*)- or (*R*)-DP glucosides **20** and **21** both ester groups are capable to maintain their typical U-shape simultaneously. The internal strain inherent to these compounds may be considered one reason why their ellagitannin analogs are not stable under physiological conditions and undergo very characteristic transformations into ring systems as realized in **11**[2] (Figs. 1 and 12; in the solid-state geometry of **11** the ester U-shape is realized in both the 2-OCO and 4-OCO linkages). However, the structure of Geraniin **11**, and the stereochemical course of this process indicates, that 2,4-*O*-(*R*)-HHDP units are the precursors rather than (*S*)-HHDP diastereomers.[2] The observation that these (*R*)-HHDP intermediates have to play an important role along the biochemical pathways of some ellagitannins correlates well with the observed stability of 2,4-*O*-(*R*)-DP glucosides over the corresponding (*S*)-DP geometries.

3. Conclusion

Without exception, the calculated relative thermodynamic stabilities of the atropdiastereomeric methyl 2,3-, 4,6-, 3,6-, and 2,4-*O*-DP-β-D-glucosides **14**–**21** correlate with the configuration of the corresponding naturally occurring HHDP-bridged ellagitannins,[2] i.e. the 2,3- and 4,6-*O*-(*S*)-DP, as well as the 3,6- and 2,4-*O*-(*R*)-DP glucosides are more stable than their diastereomers. The molecular modeling data and the calculated energy differences are consistent with limited flexibility of bis-equatorial linked DP-residues in 2,3- and 4,6-positions of D-glucose ($^4C_1$ pyranose conformation), the 10-membered ring in the 2,3-*O*-DP glucosides being less flexible than the 11-membered 4,6-*O*-DP macrocycle with one additional CH_2-group. Even more rigid are the bis-axial linked 3,6-*O*- and 2,4-*O*-DP glucosides with $^1C_4$ glucose *anti*-chair geometries, the latter bearing even so much internal strain that they immediately undergo ensuing biochemical transformations under physiological conditions (vide supra).[2] Comparison of the calculated structures with the few solid-state structures available for **11**, **13**, and **22** attests to the consistency of the methodology applied. The strait-jacket of the carbohydrate scaffold exerts a strong chiral induction onto the attached diphenoyl-residues in all types of linkages discussed within this study, the major effect in chirality transduction emerging from the tendency of the ester groups to maintain their characteristic U-shape. Indeed, preliminary results indicate that the atropchiral induction is significantly weakened or even inverted[27] when replacing the -COO-ester groups with -CH_2-O-type linkages. As detailed for the non-natural methyl 4,6-*O*-DP galactosides **23** and **24**, the configuration of the DP-units is highly sensitive towards changes in the linkage type and/or geometry.

On the basis of the molecular geometries discussed here, not only molecular models for the various ellagitannins can be derived, but also the configuration of the HHDP-units found in the class of ellagitannins can be rationalized. Although biosynthesis of the ellagitannins proceeds via HHDP ring formation through oxidative coupling of galloyl residues, and thus the strain inherent to the transition states of ring closure is the decisive kinetic factor for the atropdiastereoselective formation of (*S*)- or (*R*)-HHDP ellagitannins, the transitions states may somewhat 'resemble' the final ellagitannin products. For this reason, the obvious build-up of torsional strain in one of the corresponding diastereomers each is apt to explain the very uniform patterns of HHDP-configurations found in the natural ellagitannins.

Oxidation of the ellagitannins at C-1 (→gluconolactons) and subsequent strain-induced pyranose ring opening[10] leads to open-chain tannins such as the Lagerstannin A, B, and C.[28] We hope to report on their geometries and conformational preferences in the near future.

4. Experimental

4.1. Crystal structures, fitting, and molecular graphics

The solid-state structures of Geraniin **11**,[19] **13**,[20] and **22**[24] were extracted from the Cambridge Crystallographic Database.[18] Hydrogen atoms not included in the structure determinations or disordered positions were positioned geometrically. 3D-fitting of molecular geometries was carried out by rigid-body translation and rotation, considering all equivalent non-hydrogen atoms with equal weights. All molecular graphics were generated using the MolArch+ program.[29]

4.2. Molecular dynamics (MD) and molecular mechanics (MM)

All MD and MM calculations were carried out using the PIMM91 force-field[30] without the explicit incorporation of solvent molecules. All starting geometries of compounds **14**–**21** were generated using the MolArch+ program,[29] different starting geometries for **16** and **17** were used to ensure the self-consistency of the search procedure for the global energy-minimum structures. For each compound, 500 ps MD trajectories were generated (time step $\Delta t = 0.5$ fs, $T = 300$ K), and molecular configurations were saved every 200 steps. Monitoring the glucopyranose geometries, as well as torsion angles along the DP-ring systems was used to ensure comprehensive coverage of the conformational space by the MD runs. For each compound **14**–**21**, a total of 5000 MD snapshot conformations were subjected to full MM energy minimization, and the global energy-minimum conformations found in each case were used in this report, and all geometry parameters (cf. Fig. 2) listed in Table 1 were calculated from this data set.[29] It is noteworthy, that the global energy-minimum structures were found multiple times in all cases, and that most of the low energy conformers within a range of 0–5 kJ/mol cluster into the same conformational family as the most stable geometry (for example, see Fig. 7).

References

1. Part 28 of the series Molecular Modelling of Saccharides. For Part 27, see: Immel, S.; Nakagawa, T.; Lindner, H.-J.; Lichtenthaler, F. W. *Chem. Eur. J.* **2000**, *6*, in press.
2. For a review, see: Quideau, S.; Feldmann, K. S. *Chem. Rev.* **1996**, *96*, 475–503.
3. Nonaka, G.-I.; Ishimatsu, M.; Ageta, M.; Nishioka, I. *Chem. Pharm. Bull.* **1989**, *37*, 50–53.
4. Tanaka, T.; Kirahara, S.; Nonaka, G.-I.; Nishioka, I. *Chem. Pharm. Bull.* **1993**, *41*, 1708–1716.
5. Feldmann, K. S.; Smith, R. S. *J. Org. Chem.* **1996**, *61*, 2606–2612.
6. Khanbabaee, K.; Lötzerich, K. *J. Org. Chem.* **1998**, *63*, 8723–8728.
7. Khanbabaee, K.; Lötzerich, K. *Liebigs Ann./Recueil* **1997**, 1571–1575.
8. Khanbabaee, K.; Lötzerich, K.; Borges, M.; Großer, M. *J. Prakt. Chem.* **1999**, *341*, 159–166.
9. Khanbabaee, K.; Schulz, C.; Lötzerich, K. *Tetrahedron Lett.* **1997**, *38*, 1367–1368.
10. Khanbabaee, K.; Lötzerich, K. *Eur. J. Org. Chem.* **1999**, 3079–3083.
11. (a) Schmidt, O. T.; Schmidt, D. M.; Herok, J. *Liebigs Ann. Chem.* **1954**, *587*, 67–74. (b) Schmidt, O. T.; Blinn, F.; Lademann, R. *Liebigs Ann. Chem.* **1952**, *576*, 75–84. (c) Schmidt, O. T.; Schmidt, D. M. *Liebigs Ann. Chem.* **1952**, *578*, 31–33.
12. Haddock, E. A.; Gupta, R. K.; Haslam, E. *J. Chem. Soc., Perkin Trans. 1* **1982**, 2535–2345.
13. Okuda, T.; Yoshida, T.; Hatano, T. *J. Chem. Soc., Perkin Trans. 1* **1982**, 9–14.
14. Tanaka, T.; Nonaka, G.-I.; Nishioka, I.; Miyahara, K.; Kawasaki, T. *J. Chem. Soc., Perkin Trans. 1* **1986**, 369–376.
15. Gupta, R. K.; Al-Shafi, S. M. K.; Layden, K.; Haslam, E. *J. Chem. Soc., Perkin Trans. 1* **1982**, 2525–2534.

16. Haslam, E. *Prog. Chem. Org. Nat. Prod.* **1982**, *41*, 1–46.
17. The proposed models for the transition states of the galloyl coupling reaction of 4,6-di-*O*-galloyl glucose (→4,6-*O*-HHDP ellagitannins) correlate the preferred formation of (*S*)-HHDP entities with conformational strain energy in the intermediates leading to the (*R*)-HHDP ellagitannins.[2] However, for both transition states, the *tg*-forms[22] of the glucose 6-CH_2O-galloyl residues were assumed. Although these rotamers frequently emerge from force-field calculations as the most stable ones, the *tg*-form is in fact the least populated state for D-glucose and its derivatives,[22,23] and does not play any significant role in glucose chemistry. The postulated transition states for the formation of 2,3-*O*-HHDP ellagitannins are almost equal in energy with very similar interatomic distances between the decisive galloyl carbon atoms, and strain is built up only in the final products.[2] To the best of our knowledge, no models for the formation of 3,6-*O*- or 2,4-*O*-HHDP ellagitannins have been put forth on an atomic level. The Monte-Carlo (MC) simulations described in Ref. 2 also did not allow to carry out a comprehensive geometry analysis of the complex fused ring systems of the ellagitannins.
18. Allen, F. H.; Kennard, O. *Chem. Des. Automat. News* **1993**, *8*, 1, 31–37; Cambridge Crystallographic Data File (Oct. 1999), Version 5.18. Refcodes: SAQZUF[19] and TASQOT.[20]
19. Luger, P.; Weber, M.; Kashino, S.; Amakura, Y.; Yoshida, T.; Okuda, T.; Beurskens, G.; Dauter, Z. *Acta Crystallogr., Sect. B* **1998**, *54*, 687–694.
20. Itoh, T.; Chika, J.; Shirakami, S.; Ito, H.; Yoshida, T.; Kubo, Y.; Uenishi, J. *J. Org. Chem.* **1996**, *61*, 3700–3705; erroneously the mirror image geometry of **13** is filed in the CCDF.
21. (a) Cremer, D. A.; Pople, J. A. *J. Am. Chem. Soc.* **1975**, *97*, 1354–1358. (b) Jeffrey, G. A.; Taylor, R. *Carbohydr. Res.* **1980**, *81*, 182–183.
22. In carbohydrate nomenclature, the three staggered conformations of the glucopyranose 6-CH_2OH groups are denoted *gauche–gauche* (*gg*), *gauche–trans* (*gt*), and *trans–gauche* (*tg*). The first letter refers to the position of O-6 relative to O-5, the second relative to C-4; the torsion angle ω is defined through the atoms O_5–C_5–C_6–O_6. For glucose, the *gg*- and *gt*-rotamers are equally preferred over *tg*, which is destabilized by 1,3-diaxial like interactions between O-6 and O-4.[23] For the C-4 epimer galactose, the conformers are populated in the order $gt \approx tg > gg$ (Scheme 1).
23. (a) Jeffrey, G. A.; Saenger, W. *Hydrogen Bonding in Biological Structures*; Springer-Verlag: Berlin/New York, 1991. (b) Kroon-Batenburg, L. M. J.; Kroon, J. *Biopolymers* **1990**, *29*, 1243–1248. (c) Bock, K.; Duus, J. Ø. *J. Carbohydr. Chem.* **1994**, *13*, 513–543.
24. Yang, D.; Yip, Y.-C.; Tang, M.-W.; Wong, M.-K.; Zheng, J.-H.; Cheung, K.-K. *J. Am. Chem. Soc.* **1996**, *118*, 491–492.
25. To the best of our knowledge, D-galactose or D-mannose derived ellagitannins are not known to occur in nature; but we envisage their chemical synthesis as an interesting target.
26. The six examples of 3,6-anhydro glycosides contained in the CCDF[18] invariably display almost undistorted $^1C_4$ *anti*-chair geometries of their pyranose portions.
27. Preliminary results indicate that for the 2,2′-bismethylenbiphenyl analogs of methyl 4,6-*O*-diphenoyl-β-D-glucoside (-COO-linkages→-CH_2O-) the (*R*)-atropisomers are preferred over the (*S*)-forms.
28. Tanaka, T.; Tong, H.-H.; Xu, Y.-M.; Ishimaru, K.; Nonaka, G.-I.; Nishioka, I. *Chem. Pharm. Bull.* **1992**, *40*, 2975–2980.
29. Immel, S. *MolArch$^+$: Molecular Architecture Modeling Program*; Darmstadt University of Technology, 2000.
30. Lindner, H. J.; Kroeker, M. *PIMM91-Closed Shell PI-SCF-LCAO-MO-Molecular Mechanics Program*; Darmstadt University of Technology, 1997. Smith, A. E.; Lindner, H. J. *J. Comput.-Aided Mol. Des.* **1991**, *5*, 235–262.